Free Convection over a Vertical Plate in a Micropolar Fluid

Subjected to a Step Change in Surface Temperature

Azizah Mohd. Rohni

Physical Science, College of Arts and Sciences

Universiti Utara Malaysia

06010 UUM, Kedah, Malaysia

Tel: 60-4-928-6980   E-mail: r.azizah@uum.edu.my

Zurni Omar (Corresponding author)

Physical Science, College of Arts and Sciences

Universiti Utara Malaysia

06010 UUM, Kedah, Malaysia

Tel: 60-4-928-6917   E-mail: zurni@uum.edu.my

Adyda Ibrahim

Physical Science ,College of Arts and Sciences

Universiti Utara Malaysia

06010 UUM, Kedah, Malaysia

Tel: 60-4-928-6956   E-mail: adyda@uum.edu.my

Abstract

The Keller box method has been employed   for free convection over a vertical plate subjected to a step change in surface temperature in micropolar fluid. Numerical results presented include the reduced angular velocity   profiles, development of wall shear stress or skin friction and development of the rate of change of the gyration component at the wall for various values of Prandtl numbers and temperature ratios. The study shows that the present results obtained in micropolar fluids, when temperature ratio $\theta_{w2} = 1$, agree very well with the previous study without temperature change.

Keywords: Keller box, Free convection, Vertical plate, Step change, Micropolar fluid

1. Introduction

Free convection or (natural convection) is a process whereby the fluid motion is induced by buoyancy forces within the fluid. The mechanism of free or natural convection flow is a buoyancy-induced motion due to the presence of a fluid density gradient and a body force that is proportional to density. The phenomenon is of great importance in industries and the environment, such as materials processing and solar energy system.

Since the first successful experimental and theoretical study of a flat plate with uniform wall temperature by Schmidt and Beckmann, free convection heat transfer from a vertical flat plate in a quiescent medium has been studied by many investigators (Lee &Yovanovich,1987a). Ostrach (1953) solved laminar boundary layer equations through similarity methods for the case of uniform wall temperature for various Prandtl numbers. Similarity solutions to boundary layer equations have been further extended by Sparrow and Gregg (1958). They have documented the results for the cases of surface temperature variations of the power-law and exponential form.

The above cited literature and many others deal with similarity problems with continuous and well-behaved boundary conditions at the wall. However, most practical problems in application often involve wall conditions that are arbitrary and unknown. The study of non-similar free convection heat transfer from a vertical flat plate with arbitrarily varying thermal conditions at the wall is a tedious investigation. The problem has attracted a great deal of interest over the past

years in several technological applications, particularly in the thermal design of microelectronic circuit boards and in the consideration of system behaviour under conditions where the usual mode of heat transfer fails.

To understand and solve problems involving general non-similar conditions at the wall, it is useful to investigate problems subjected to a step change in wall temperature (Lee &Yovanovich,1987b). The problems impose a mathematical singularity and severe non-similar conditions at the wall.

2. Governing Equations

We consider a semi-infinite vertical heated plate with a discontinuous temperature variation immersed in a micropolar fluid. It is well known that the full equations governing the steady laminar free convection flow of an incompressible micropolar fluid subject to Boussinesq approximation may be written in the form

$$\frac{\partial \overline{u}}{\partial \overline{x}} + \frac{\partial \overline{v}}{\partial \overline{y}} = 0,$$

(1)

$$\rho\left(\overline{u}\frac{\partial \overline{u}}{\partial \overline{x}} + \overline{v}\frac{\partial \overline{u}}{\partial \overline{y}}\right) = -\frac{\partial \overline{p}}{\partial \overline{x}} + (\mu+\kappa)\left(\frac{\partial^2 \overline{u}}{\partial \overline{x}^2} + \frac{\partial^2 \overline{u}}{\partial \overline{y}^2}\right) + \rho g \beta (T - T_\infty) + \kappa\frac{\partial \overline{N}}{\partial \overline{y}},$$

(2)

$$\rho\left(\overline{u}\frac{\partial \overline{v}}{\partial \overline{x}} + \overline{v}\frac{\partial \overline{v}}{\partial \overline{y}}\right) = -\frac{\partial \overline{p}}{\partial \overline{y}} + (\mu+\kappa)\left(\frac{\partial^2 \overline{v}}{\partial \overline{x}^2} + \frac{\partial^2 \overline{v}}{\partial \overline{y}^2}\right) - \kappa\frac{\partial \overline{N}}{\partial \overline{x}},$$

(3)

$$\rho j\left(\overline{u}\frac{\partial \overline{N}}{\partial \overline{x}} + \overline{v}\frac{\partial \overline{N}}{\partial \overline{y}}\right) = -2\kappa\overline{N} + \kappa\left(\frac{\partial \overline{v}}{\partial \overline{x}} - \frac{\partial \overline{u}}{\partial \overline{y}}\right) + \gamma\left(\frac{\partial^2 \overline{N}}{\partial \overline{x}^2} + \frac{\partial^2 \overline{N}}{\partial \overline{y}^2}\right),$$

(4)

$$\overline{u}\frac{\partial T}{\partial \overline{x}} + \overline{v}\frac{\partial T}{\partial \overline{y}} = \alpha\left(\frac{\partial^2 T}{\partial \overline{x}^2} + \frac{\partial^2 T}{\partial \overline{y}^2}\right),$$

(5)

where $(\overline{u}, \overline{v})$ are the velocity components along the $(\overline{x}, \overline{y})$ axes; T, $\overline{p}$ and $\overline{N}$ are the temperature, pressure and the component of the gyration vector normal to the (x, y)- plane; g is the acceleration due to gravity; ρ, μ, α and β are the fluid density, viscosity, thermal diffusity and coefficient of cubical expansion of the fluid; j, κ and γ are the micro inertia density, vortex viscosity and spin gradient viscosity. Also, $v = \frac{\mu}{\rho}$ is the kinematic viscosity. The spin gradient viscosity is given by the constant

$$\gamma = (\mu + \kappa/2) j.$$

(6)

The governing equations are subject to the following boundary conditions:

$$\overline{y} = 0 \quad : \quad \overline{u} = \overline{v} = 0, \overline{N} = -n\frac{\partial \overline{u}}{\partial \overline{y}},$$

$$T = T_{w1} \text{ for } \overline{x} \leq \overline{x}_0 \text{ and } T = T_{w2} \text{ for } \overline{x} > \overline{x}_0,$$

$$\overline{y} \to \infty \quad : \quad \overline{u} \to 0, \overline{v} \to 0, \overline{N} \to 0, T \to T_\infty.$$

(7)

It is worth mentioning that in (7), we have followed [1] for temperature condition.

Equations 1-5 may be written dimensionless by introducing the non-dimensional variables:

$$(\overline{u}, \overline{v}) = (g\beta\Delta Tl)^{\frac{1}{2}} (u, v), \quad (\overline{x}, \overline{y}) = l(x, y)$$

$$\overline{p} = (g\beta\Delta Tl)\rho p, \quad T = T_\infty + \Delta T\theta, \quad N = (g\beta\Delta T/l)^{\frac{1}{2}} N,$$

(8)

where $j = l^2$ is the length scale for l and $\Delta T = T_w - T_\infty$.

So, the governing equations 1-5, after being rendered dimensionless are as follows

$$\frac{\partial u}{\partial x} + \frac{\partial v}{\partial y} = 0,$$

(9)

$$u\frac{\partial u}{\partial x} + v\frac{\partial u}{\partial y} = -\frac{\partial p}{\partial x} + \left(\frac{1+K}{\mathrm{Gr}^{\frac{1}{2}}}\right)\left(\frac{\partial^2 u}{\partial x^2} + \frac{\partial^2 u}{\partial y^2}\right) + \theta + \frac{K}{\mathrm{Gr}^{\frac{1}{2}}}\frac{\partial N}{\partial y},$$

(10)

$$u\frac{\partial v}{\partial x} + v\frac{\partial v}{\partial y} = -\frac{\partial p}{\partial y} + \left(\frac{1+K}{Gr^{\frac{1}{2}}}\right)\left(\frac{\partial^2 v}{\partial x^2} + \frac{\partial^2 v}{\partial y^2}\right) - \frac{K}{Gr^{\frac{1}{2}}}\frac{\partial N}{\partial x},$$

(11)

$$u\frac{\partial N}{\partial x} + v\frac{\partial N}{\partial y} = -2\frac{K}{Gr^{\frac{1}{2}}}N + \frac{K}{Gr^{\frac{1}{2}}}\left(\frac{\partial v}{\partial x} - \frac{\partial u}{\partial y}\right) + \left(\frac{1+\frac{1}{2}K}{Gr^{\frac{1}{2}}}\right)\left(\frac{\partial^2 N}{\partial x^2} + \frac{\partial^2 N}{\partial y^2}\right),$$

(12)

$$u\frac{\partial \theta}{\partial x} + v\frac{\partial \theta}{\partial y} = \frac{1}{\Pr Gr^{\frac{1}{2}}}\left(\frac{\partial^2 \theta}{\partial x^2} + \frac{\partial^2 \theta}{\partial y^2}\right),$$

(13)

where $K = \dfrac{\kappa}{\mu}$ is the material parameter, $\mathrm{Gr} = \dfrac{g\beta\Delta T l^3}{v^2}$ is the Grashof number and $\Pr = \dfrac{v}{\alpha}$ is the Prandtl number.

The dimensionless governing equations are subjected to the following boundary conditions:

$$y = 0 \quad : \quad u = 1, \, v = 0, \, N = -n\frac{\partial u}{\partial y},$$

$$\theta = 1 \text{ for } x \le x_0 \text{ and } \theta = \theta_{w2} \text{ for } x > x_0,$$

$$y \to \infty \; : \; u \to 0, \, v \to 0, \, N \to 0, \, \theta \to 0.$$

(14)

Next, we set the boundary layer variables

$$x = \mathrm{Gr}\hat{x}, \; y = \hat{y}, \; u = \mathrm{Gr}^{\frac{1}{2}}\frac{\partial \psi}{\partial \hat{y}}, \; v = -\mathrm{Gr}^{-\frac{1}{4}}\frac{\partial \psi}{\partial \hat{x}}, \text{ and } N = \mathrm{Gr}^{\frac{1}{4}}\hat{N}.$$

(15)

where ψ is the stream function defined in such a way that equation (9) is identically satisfied.

Hence, we substitute the variables in (15) into equations 10-13 and formally let the Grashof number become asymptotically large ($\mathrm{Gr} \to \infty$).

The set of governing equation, after introducing the boundary layer variables is

$$\frac{\partial \psi}{\partial \hat{y}}\frac{\partial^2 \psi}{\partial \hat{y}\partial \hat{x}} - \frac{\partial \psi}{\partial \hat{x}}\frac{\partial^2 \psi}{\partial \hat{y}^2} = (1+K)\frac{\partial^3 \psi}{\partial \hat{y}^3} + \theta + K\frac{\partial \hat{N}}{\partial \hat{y}},$$

(16)

$$\frac{\partial \psi}{\partial \hat{y}}\frac{\partial \hat{N}}{\partial \hat{x}} - \frac{\partial \psi}{\partial \hat{x}}\frac{\partial \hat{N}}{\partial \hat{y}} = -2K\hat{N} - K\frac{\partial^2 \psi}{\partial \hat{y}^2} + \left(1 + \frac{1}{2}K\right)\frac{\partial^2 \hat{N}}{\partial \hat{y}^2},$$

(17)

$$\frac{\partial \psi}{\partial \hat{y}}\frac{\partial \theta}{\partial \hat{x}} - \frac{\partial \psi}{\partial \hat{x}}\frac{\partial \theta}{\partial \hat{y}} = \frac{1}{\Pr}\frac{\partial^2 \theta}{\partial \hat{y}^2},$$

(18)

subjected to the boundary conditions in (14) that have been reduced to

$$\hat{y} = 0 \quad : \quad \psi = \frac{\partial \psi}{\partial \hat{y}} = 0, \, \hat{N} = -n\frac{\partial^2 \psi}{\partial \hat{y}^2},$$

$$\theta = 1 \text{ for } \hat{x} \le \hat{x}_0 \text{ and } \theta = \theta_{w2} \text{ for } \hat{x} > \hat{x}_0,$$

$$\hat{y} \to \infty \; : \; \frac{\partial \psi}{\partial \hat{y}} \to 0, \, \hat{N} \to 0, \, \theta \to 0.$$

(19)

The standard similarity form of Polhausen (1921) may be used to derive the non-similar boundary-layer equations. Therefore, we set

$$\psi = \xi^{\frac{3}{4}} f\left(\xi, \eta\right), \quad \theta = \mathrm{g}\left(\xi, \eta\right), \quad \hat{N} = \xi^{\frac{1}{4}} h\left(\xi, \eta\right), \quad \xi = \hat{x}, \quad \eta = \frac{\hat{y}}{\hat{x}^{\frac{1}{4}}}.$$

(20)

Thus, the governing equations for boundary-layer flows become

$$(1+K)\frac{\partial^3 f}{\partial \eta^3} - \frac{1}{2}\left(\frac{\partial f}{\partial \eta}\right)^2 + K\frac{\partial h}{\partial \eta} + \frac{3}{4}f\frac{\partial^2 f}{\partial \eta^2} + g = \xi\left(\frac{\partial f}{\partial \eta}\frac{\partial^2 f}{\partial \xi \partial \eta} - \frac{\partial f}{\partial \xi}\frac{\partial^2 f}{\partial \eta^2}\right),$$

(21)

$$\left(1 + \frac{1}{2}K\right)\left(\frac{\partial^2 h}{\partial \eta^2}\right) + \frac{3}{4}f\frac{\partial h}{\partial \eta} - \frac{1}{4}h\frac{\partial f}{\partial \eta} = \xi\left(\frac{\partial f}{\partial \eta}\frac{\partial h}{\partial \xi} - \frac{\partial f}{\partial \xi}\frac{\partial h}{\partial \eta}\right) + K\xi^{\frac{1}{2}}\left(2h + \frac{\partial^2 f}{\partial \eta^2}\right),$$

(22)

$$\frac{1}{\mathrm{Pr}}\frac{\partial^2 g}{\partial \eta^2} + \frac{3}{4}f\frac{\partial g}{\partial \eta} - = \xi\left(\frac{\partial f}{\partial \eta}\frac{\partial g}{\partial \xi} - \frac{\partial f}{\partial \xi}\frac{\partial g}{\partial \eta}\right),$$

(23)

with the boundary conditions

$$\eta = 0 \quad : \quad f = \frac{\partial f}{\partial \eta} = 0, \quad h + n\frac{\partial^2 f}{\partial \eta^2} = 0,$$

$$g = 1 \text{ for } x \leq x_0 \text{ and } g = g_{w2} \text{ for } x > x_0,$$

$$\eta \to \infty \quad : \quad \frac{\partial f}{\partial \eta} \to 0, \; h \to 0, \; g \to 0.$$

(24)

Equations 21-23 subject to (24) should be solved for different values of ξ with n in the range of $0 \leq n \leq 1$ using the Keller-Box scheme. Before that, we need to introduce $X = \xi^{\frac{1}{2}}$, so that the equations can be written as

$$(1+K)\frac{\partial^3 f}{\partial \eta^3} - \frac{1}{2}\left(\frac{\partial f}{\partial \eta}\right)^2 + K\frac{\partial h}{\partial \eta} + \frac{3}{4}f\frac{\partial^2 f}{\partial \eta^2} + g = \frac{1}{2}X\left(\frac{\partial f}{\partial \eta}\frac{\partial^2 f}{\partial X \partial \eta} - \frac{\partial f}{\partial X}\frac{\partial^2 f}{\partial \eta^2}\right),$$

(25)

$$\left(1 + \frac{1}{2}K\right)\left(\frac{\partial^2 h}{\partial \eta^2}\right) + \frac{3}{4}f\frac{\partial h}{\partial \eta} - \frac{1}{4}h\frac{\partial f}{\partial \eta} = \frac{1}{2}X\left(\frac{\partial f}{\partial \eta}\frac{\partial h}{\partial X} - \frac{\partial f}{\partial X}\frac{\partial h}{\partial \eta}\right) + KX\left(2h + \frac{\partial^2 f}{\partial \eta^2}\right),$$

(26)

$$\frac{1}{\mathrm{Pr}}\frac{\partial^2 g}{\partial \eta^2} + \frac{3}{4}f\frac{\partial g}{\partial \eta} - = \frac{1}{2}X\left(\frac{\partial f}{\partial \eta}\frac{\partial g}{\partial X} - \frac{\partial f}{\partial X}\frac{\partial g}{\partial \eta}\right).$$

(27)

The reason is that the factor $\xi^{\frac{1}{2}}$ will cause large errors at the beginning of computation.

Boundary layer equations 25-27 subject to the boundary conditions (24) are solved numerically using the Keller-box method. In this method, the governing equations are first reduced to first order equation. We use the Newton's method to linearise the resulting nonlinear equations and finally, we obtain the solutiond using the block elimination methods

3. Numerical Solution

The results obtained by using Keller box method for the problem considered are presented here in. Comparison between present results and the existing solution in the literature is also included. The new results obtained by using Keller box method include the reduced angular velocity profiles, development of wall shear stress or skin friction and development of the rate of change of the gyration component at the wall for various values of θ_{w2}. To assess the accuracy of the present results, comparisons between the present results and previously published data reported by Rees & Pop (1997) are made.

4. Conclusion

From this study we can draw the following conclusions:

• In the cases of fixed K and n, the reduced angular velocity increases then decreases with increasing Prandtl number and eventually tends to zero.

- For fixed K and n , wall shear stress decreases then increases and eventually tends to zero with an increase in Prandtl number.

- For fixed K and n the rate of heat transfer increases then decreases and increases again and eventually tends to zero with an increase in Prandtl number.

References

Kelleher, M. (1971). Free Convection From A Vertical Plate With Discontinous Wall Temperature. *Trans. ASME*, 93, 349-356.

Lee, S. & Yovanovich, M.M. (1987a). Laminar Natural Convection From A Vertical Plate With Variations In Wall Temperature. *Journal of Heat Transfer*, 113, 111-119.

Lee, S. & Yovanovich, M.M. (1987b). Laminar Natural Convection From A Vertical Plate With A Step Change In Wall Temperature. *Journal of Heat Transfer*, 113, 501-504.

Ostrach, S. (1953). An Analysis of Laminar Free-Convection Flow and Heat Transfer about a Flat Plate Parallel to the Direction of the Generating Body Forces. *NACA TR,* 1111.

Rees, D.A.S & Pop. I. (1997). Free Convection Boundary Layer Flow of a Micropolar Fluid From a Vertical Flat Plate. *Journal of Applied Mathematics,* 61, 179-197

Sparrow, E.M. and Gregg, J.L. (1958). Similar Solutions for Free Convection From a Nonisothermal Vertical Plate*, Trans. ASME*., 80, 379-386.

Table 1. Comparison between Rees & Pop (1998) and the present method for variation of $h(0)$, $h'(0)$ and $g'(0)$

Pr	$h(0)$		$h'(0)$		$g'(0)$	
	Rees & Pop (1998)	Current	Rees & Pop (1998)	Current	Rees & Pop (1998)	Current
0.1	- 1.21505	- 1.21511	0.71152	0.71160	- 0.16274	- 0.16272
0.2	- 1.13288	- 1.13301	0.63528	0.63542	- 0.21772	- 0.21771
0.5	- 1.00855	- 1.00866	0.52277	0.52282	- 0.31195	- 0.31195
0.7	- 0.96012	- 0.96022	0.48000	0.48007	- 0.35321	- 0.35321
1.0	- 0.90819	- 0.90827	0.43495	0.43501	- 0.40103	- 0.40105
2.0	- 0.80789	- 0.80794	0.35117	0.35121	- 0.50662	- 0.50666
5.0	- 0.68135	- 0.68140	0.25424	0.25427	- 0.67458	- 0.67470
6.7	- 0.64312	- 0.64316	0.22741	0.22745	- 0.73597	- 0.73613
10.0	- 0.59283	- 0.59287	0.19411	0.19415	- 0.82684	- 0.82709

Table 1 shows that the solution obtained using the present method is remarkably close to the existing solution by Rees & Pop (1997).
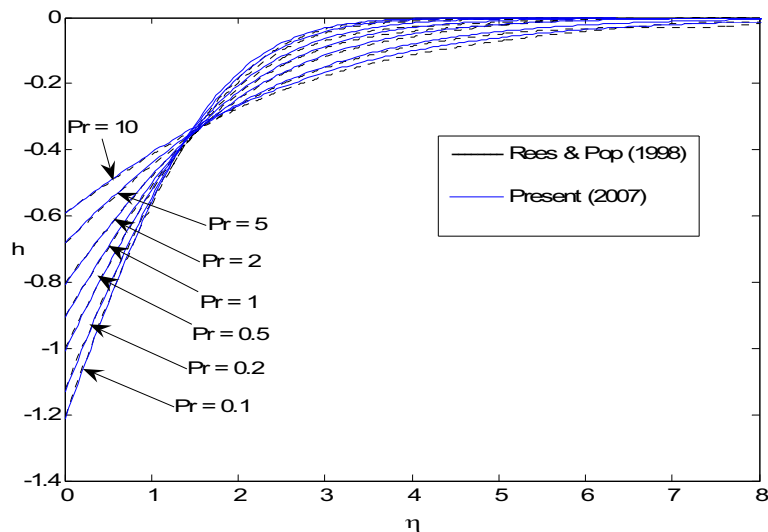
Figure 1. Comparison between Rees & Pop (1998) and the

present method for profiles of the reduced angular

velocity *h* as a function of η for different values of

Pr when $K = 0$ and $n = 1$.

As we can see from the Figure 1, it is shown that the agreement between present results and those obtained by Rees & Pop are very good. Therefore, we confident that the present results are accurate. Hence, this is an encouragement to further study this problem.
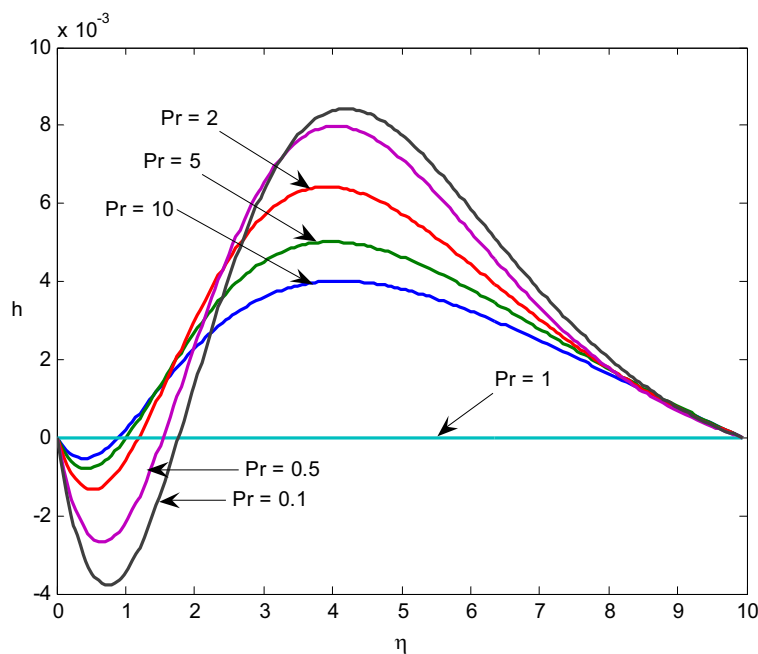

Figure 2. Profiles of the reduced angular velocity *h* as a

function of η for different values of Pr
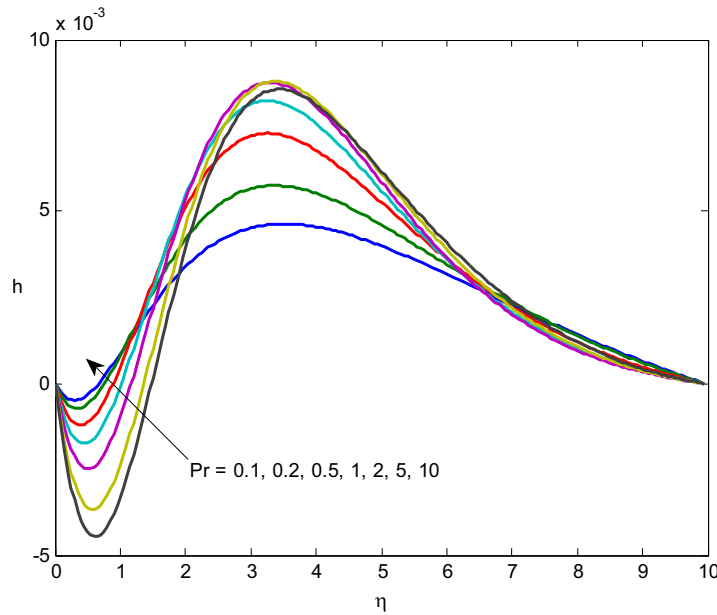
when $K = 1$, $n = 0$ and $\theta_{w2} = 0.5$.

Figure 3. Profiles of the reduced angular velocity h
as a function of η for different values of Pr
when $K = 1$, $n = 0$ and $\theta_{w2} = 2$.
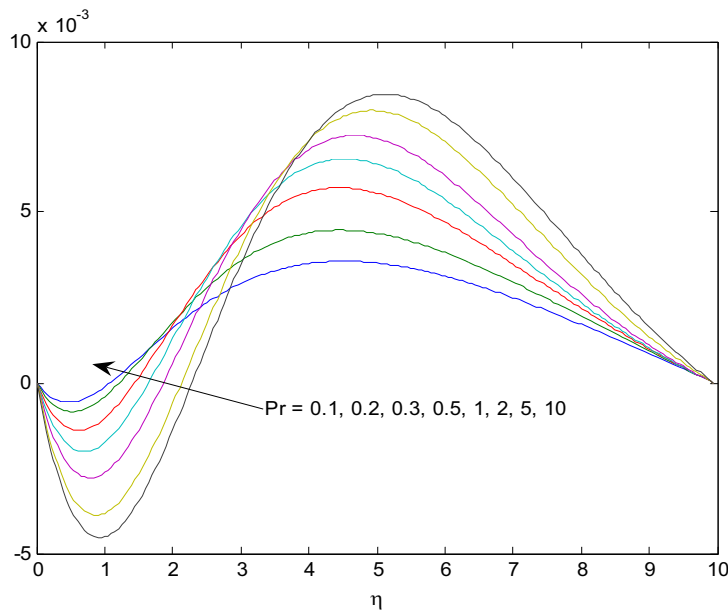
Figure 4. Profiles of the reduced angular velocity h as a function of η for
different values of Pr when $K = 1$, $n = 0$ and $\theta_{w2} = 0$.

In Figures 2-4, we have shown some graphs of the characteristics of angular velocity profile as a function of η at different streamwise locations for $\theta_{w2} = 0.5, 2$ and 0. Figures 2-4 show that h initially increases then decreases and eventually tends to zero with an increase in Pr.
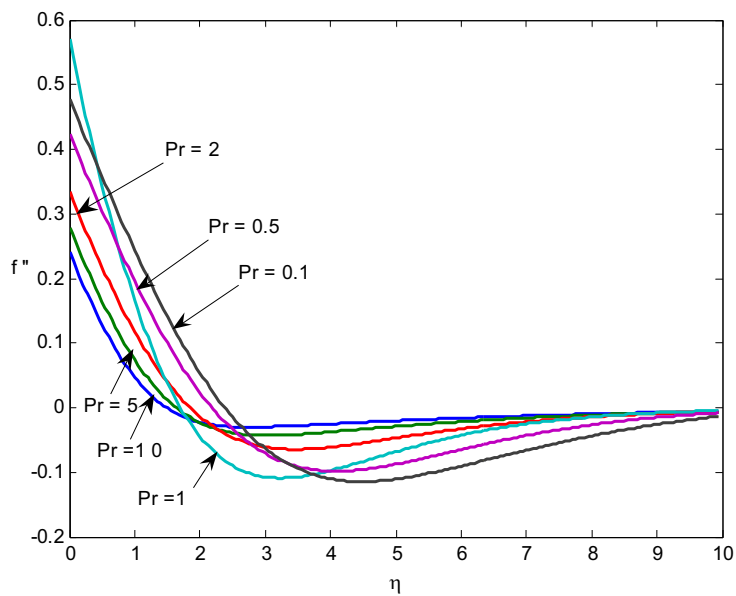
Figure 5. Profiles of the shear stress f'' as a function of η for different values of Pr when $K = 1$, $n = 0$ and $\theta_{w2} = 0.5$.
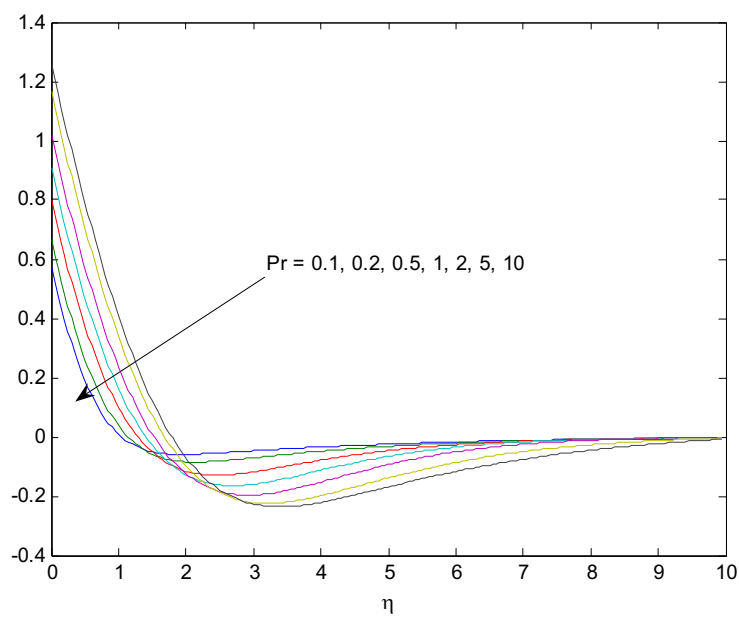

Figure 6. Profiles of the shear stress f'' as a function of η for different values of Pr when $K = 1$, $n = 0$ and $\theta_{w2} = 2$.
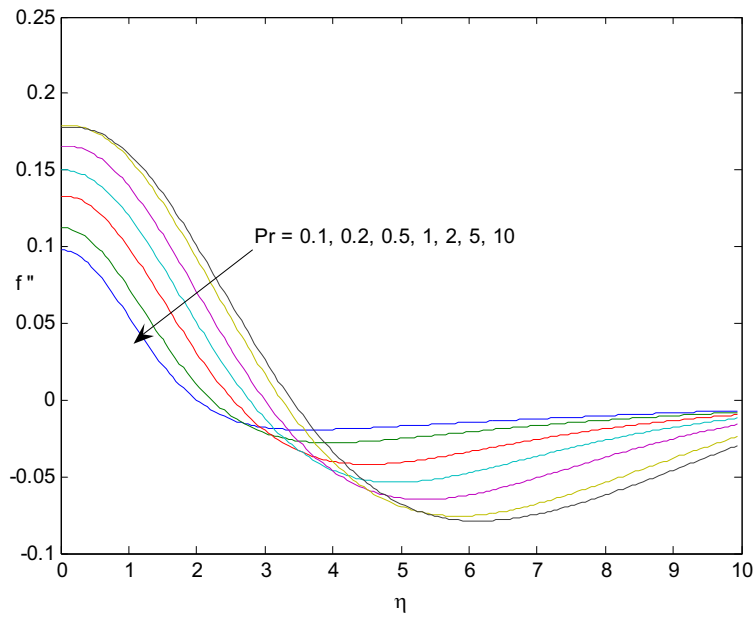
Figure 7. Profiles of the shear stress f'' as a function of η for different values of Pr when $K = 1$, $n = 0$ and $\theta_{w2} = 0$.
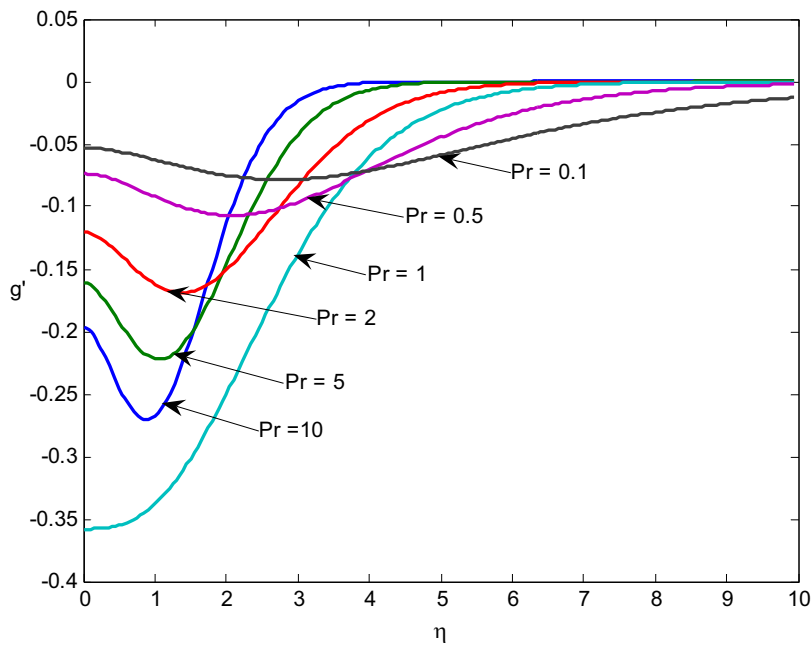

Figure 8. Profiles of rate of heat transfer g' as a function of η for different values of Pr when $K = 1$, $n = 0$ and $\theta_{w2} = 0.5$.
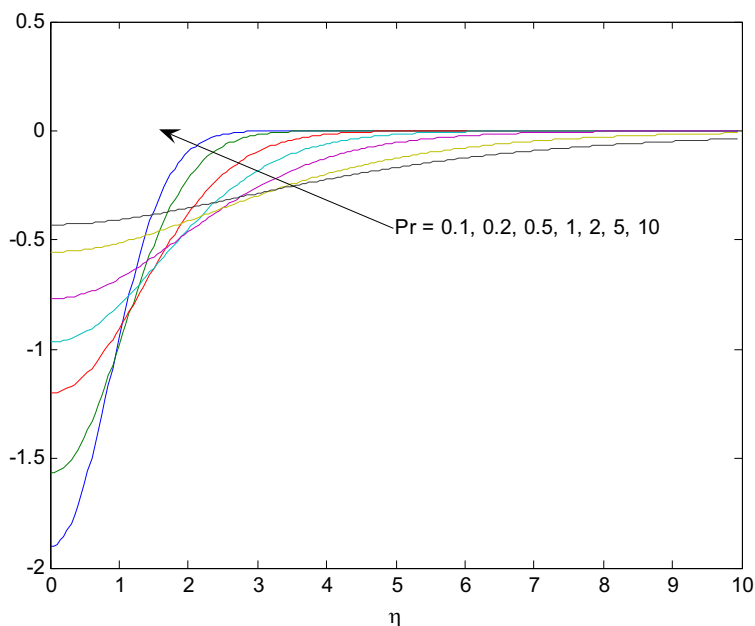
Figure 9. Profiles of rate of heat transfer g' as a function of η for different
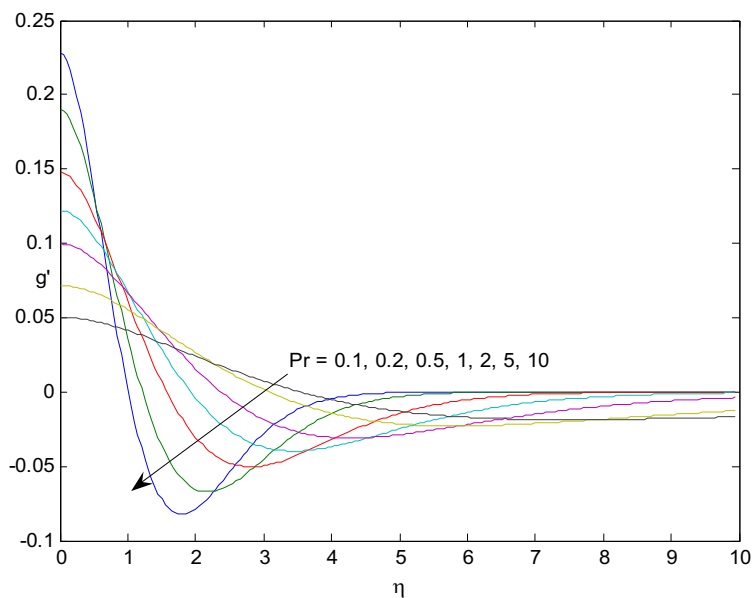values of Pr when $K = 1$, $n = 0$ and $\theta_{w2} = 2$.

Figure 10. Profiles of rate of heat transfer g' as a function of η for
different values of Pr when $K = 1$, $n = 0$ and $\theta_{w2} = 0$.

From Figures 5-10, we now consider the variation of the shear stress (or skin friction) and the rate of change of gyration component at the solid boundary with η. From Figure 4 and Figure 7, we show f'' as a function of η at different streamwise locations for $\theta_{w2} = 0.5$, 2 and 0. Figures 4-7 show that f'' decreases then increases and eventually tends to zero with an increase in Pr. Otherwise, Figures 8-10 show g' increases then decreases and increases again and eventually tends to zero.